

PARTONIC INTERPRETATION OF DIFFRACTION AT HERA*

CHRISTIAN KIESLING

Max-Planck-Institut für Physik
Föhringer Ring 6, 80801 München, Germany

(Received November 29, 2004)

We present the data on diffractive scattering in electron–proton reactions at HERA and review the analysis of these data in terms of diffractive parton distribution functions. From these a clear picture of the partonic structure of diffractive exchange emerges. The basis of the analysis is the factorization property of diffractive exchange, which is subjected to experimental tests using deep-inelastic diffractive charm and jet production, as well as photoproduction of jets.

PACS numbers: 12.38.Aw, 12.38.Bx, 12.39.St

1. Introduction

Quantum Chromodynamics (QCD) is expected to describe the strong interactions between quarks and gluons. At distances small compared to the nucleon radius, or equivalently large momentum transfer Q^2 where the strong coupling constant α_s is small, perturbative QCD (pQCD) gives an adequate quantitative account of hadronic processes. The total cross sections for high energy reactions, however, are usually dominated by long range forces (“soft interactions”), where a satisfactory understanding of QCD still remains a challenge. A large fraction of these soft interactions, characterized by an almost energy-independent cross section, are mediated by color-singlet (vacuum quantum number) exchange, and are termed “*diffractive*”. In hadronic interactions, diffraction is well described by Regge theory, which is formalized as a t -channel exchange of a leading trajectory with vacuum quantum numbers, called the “Pomeron” trajectory. In the high energy limit, Pomeron exchange dominates over all other contributions to the scattering amplitude and thus represents an essential feature of strong interactions. In

* Presented at the XXXIV International Symposium on Multiparticle Dynamics, Sonoma County, California, USA, July 26–August 1, 2004.

recent years there has been considerable interest in studying “hard diffraction” in order to understand the exchange at the parton level.

The electron–proton collider HERA is an ideal place to study hard diffraction in deep-inelastic scattering (DIS) and, therefore, provides powerful new experimental input to study the strong interaction of hadrons. Since the high-energy limit of virtual-photon proton reactions is equivalent to the low Bjorken x regime in DIS, gluons are expected to dominate the diffractive exchange.

Hard diffraction at HERA is a unique tool to investigate the partonic structure of diffractive exchange. Fig. 1 sketches the generic diffractive process in electron–proton scattering at HERA, displaying also the relevant kinematic variables in the virtual-photon proton reaction. The colorless exchange produces two hadronic systems M_X and M_Y , with a total invariant mass W (*i.e.* the virtual-photon proton center-of-mass energy). At high values of W the colorless exchange leads to a large rapidity gap, void of particles, which provides a unique signature for diffractive events. If the system M_Y is just the intact scattered proton, the diffractive process is called “photon-dissociation”. Such processes allow us to study in detail the partonic structure of the colorless exchange and are, therefore, the focus of this review.

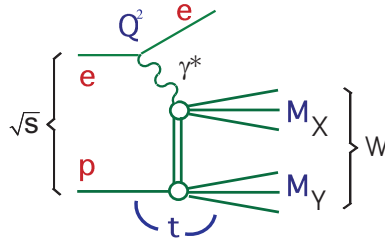


Fig. 1. Generic diagram for diffractive processes in electron–proton scattering, showing the relevant kinematic variables. The two hadronic systems X (“photon dissociation”) and Y (“proton dissociation”) with masses M_X and M_Y , respectively, are usually separated by a large rapidity gap.

2. Experimental methods

To select diffractive events coming from photon dissociation, several techniques are used by the two HERA experiments. The cleanest way to detect the scattered proton in the forward (= proton) direction is the so-called *Roman pot* technique, which employs several detectors inserted in the beam pipe forming, together with the guide field magnets of the proton accelerator, a proton spectrometer. This method was exploited by both H1 [1]

and ZEUS [2]. In addition to being free of proton dissociation, the Roman pot method gives access to a measurement of the momentum transfer t at the lower vertex (see Fig. 1). The evident drawback of this method is low statistics due to the limited acceptance of the proton spectrometers.

High statistics diffractive samples can be obtained using the characteristic properties of the hadronic final state. H1 selects the events on the basis of a large rapidity gap separating the leading baryonic system Y from the photon dissociation system X (see Fig. 1). The rapidity gap is identified by the absence of activity in detectors sensitive to the forward energy flow in the rapidity range $3.2 < \eta < 7.5$. This large empty η range ensures that photon dissociation dominates and limits the baryonic system to masses $M_Y < 1.6$ GeV. The residual proton dissociation background is about 9% and can be subtracted statistically.

ZEUS employs the so-called M_X -method, which is based on the observation that diffractive and non-diffractive final states have very different distributions in the variable $\ln M_X^2$. The invariant mass M_X is reconstructed from all observed particles in the final state, excluding the identified scattered electron. Monte Carlo simulations show that the diffractive contribution is essentially flat in $\ln M_X^2$, while the non-diffractive contribution falls off exponentially towards lower masses M_X and can thus be subtracted.

3. General features of diffraction at HERA

As explained in the previous sections, diffractive processes are characterized by a large rapidity gap which give access to an analysis of the kinematics related to the diffractive exchange, carrying a fraction x_P of the initial proton's longitudinal momentum, between the two hadronic systems M_X and M_Y (see Fig. 2).

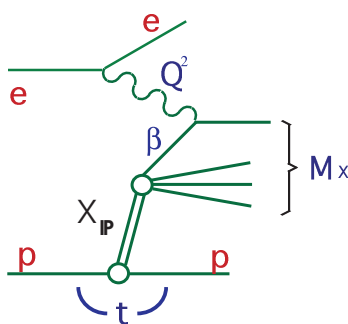


Fig. 2. Feynman diagram for deep-inelastic diffractive scattering. Neglecting the momentum transfer t and the proton mass, the following scaling variables x_P and β can be defined: $x_P = (Q^2 + M_X^2)/(Q^2 + W^2)$, $\beta = Q^2/(Q^2 + M_X^2) = x/x_P$.

The subscript \mathcal{P} reminds us of the frequently used association of diffractive exchange with the “*Pomeron*”. The variable β in turn is interpreted as the fractional longitudinal momentum carried by a charged constituent (a quark) within the Pomeron. With these additional variables, integrating over the mass of the usually unobserved hadronic system Y , the fully differential diffractive cross section σ^{D} can be defined, in analogy to the conventional deep inelastic scattering, as

$$\frac{d^4\sigma^{\text{D}}}{dx_{\mathcal{P}} dt d\beta dQ^2} = \frac{2\pi\alpha^2}{\beta Q^4} (1 + (1 - y)^2) \sigma_{\text{r}}^{\text{D}(4)}(x_{\mathcal{P}}, \beta, t, Q^2). \quad (1)$$

Here, the *reduced cross section* $\sigma_{\text{r}}^{\text{D}(4)}$ is related to the diffractive structure functions $F_2^{\text{D}(4)}$ and $F_{\text{L}}^{\text{D}(4)}$, neglecting contributions from Z^0 exchange, by

$$\sigma_{\text{r}}^{\text{D}(4)} = F_2^{\text{D}(4)} - \frac{y^2}{1 + (1 - y)^2} F_{\text{L}}^{\text{D}(4)}. \quad (2)$$

Similarly to the case of the reduced inclusive cross section, the longitudinal contribution $F_{\text{L}}^{\text{D}(4)}$ can be safely neglected, except possibly at large values of y . If the outgoing proton is not detected one has to integrate Eq. (1) over t and the experimentally accessible quantity is $x_{\mathcal{P}}\sigma_{\text{r}}^{\text{D}(3)} = \int \sigma_{\text{r}}^{\text{D}(4)} dt$.

Various phenomenological models for diffractive scattering have been formulated [3, 4]. Here we would like to follow a model-independent approach within perturbative QCD, using the concept of *diffractive parton distributions* f_i^{D} (“*dpdf's*”). The approach is based on a rigorous proof [5] to leading twist in pQCD which states that the cross section for diffractive scattering can be factorized into a short range (“hard”) part and a non-perturbative (“soft”) part. The diffractive cross section as given in Eq. (1) can, therefore, be expressed, at fixed $x_{\mathcal{P}}$ and t , as a sum of convolutions of universal hard scattering partonic cross sections $\hat{\sigma}^{\gamma^*i}$ with the non-perturbative diffractive parton densities f_i^{D} :

$$\frac{d^2\sigma^{\gamma^*p \rightarrow p'X}(x, Q^2, x_{\mathcal{P}}, t)}{dx_{\mathcal{P}} dt} = \sum_i \int_x^{x_{\mathcal{P}}} d\xi f_i^{\text{D}}(\xi, Q^2, x_{\mathcal{P}}, t) \hat{\sigma}^{\gamma^*i}(x, Q^2, \xi). \quad (3)$$

The hard-scattering cross sections $\hat{\sigma}^{\gamma^*i}$ are the same as those in inclusive deep-inelastic scattering and are calculable in pQCD. The diffractive parton distributions, as their inclusive analogues, are not known from first principles, but should evolve in Q^2 according to the DGLAP equations. Therefore, the NLO QCD framework used to extract parton densities in inclusive deep-inelastic scattering can be applied also to diffractive deep-inelastic scattering.

3.1. The Ingelman–Schlein model

Though not proven rigorously in pQCD, one may further suppose that the shapes in ξ and Q^2 of the parton distributions within the diffractive exchange, in relation (3), are independent of the kinematic quantities $x_{\mathbb{P}}$ and t . This is equivalent to the picture of a diffractive pseudo-particle exchange, the Pomeron, with a partonic structure independent of the Pomeron kinematics. With this assumption the densities f_i^{D} can be factorized into a Pomeron flux term depending only on $x_{\mathbb{P}}$ and t , and a set of parton densities, depending only on x (or $\beta = x/x_{\mathbb{P}}$) and Q^2 , characteristic for the Pomeron exchange:

$$f_i^{\text{D}}(x, Q^2, x_{\mathbb{P}}, t) = f_{\mathbb{P}/p}(x_{\mathbb{P}}, t) \cdot f_i^{\mathbb{P}}(\beta, Q^2). \quad (4)$$

This model for diffractive exchange was proposed by Ingelman and Schlein [6] and is also often called the *resolved Pomeron model*. The variable β then corresponds to the longitudinal momentum fraction of the struck parton within the Pomeron (see Fig. 2 for the lowest order diagram). The Pomeron flux factor in this model is defined as

$$f_{\mathbb{P}/p}(x_{\mathbb{P}}, t) = e^{Bt} / x_{\mathbb{P}}^{2\alpha(t)-1}, \quad (5)$$

with the usual linear Pomeron Regge trajectory $\alpha(t)$ (see [7]), and a t slope taken from the literature [8]. Correspondingly, the diffractive structure function $F_2^{\text{D}(4)}$ is then given via the Regge factorization assumption as:

$$F_2^{\text{D}(4)}(x_{\mathbb{P}}, t, \beta, Q^2) = f_{\mathbb{P}/p}(x_{\mathbb{P}}, t) F_2^{\mathbb{P}}(\beta, Q^2). \quad (6)$$

The validity of the above Regge factorization ansatz has been studied experimentally and was found to be consistent with the data for low values of $x_{\mathbb{P}}$ ($x_{\mathbb{P}} < 10^{-2}$, see below).

3.2. The data on inclusive diffractive scattering

Following the formalism outlined above, the previously published diffractive data from both HERA collaborations [9, 10], being selected along the lines described in Section 2, have been updated recently [11, 12]. The new H1 measurements include also data from 1999 and 2000, so that the high Q^2 region ($Q^2 > 120 \text{ GeV}^2$, corresponding to an integrated luminosity of 61 pb^{-1}) can now be accessed. As an example, the H1 data for the reduced diffractive cross sections $x_{\mathbb{P}}\sigma_{\text{r}}^{\text{D}(3)}$ as functions of $x_{\mathbb{P}}$ for fixed values of β and Q^2 are shown in Fig. 3 together with predictions from an NLO-QCD fit to the medium Q^2 data, to be discussed below. For this measurement the data

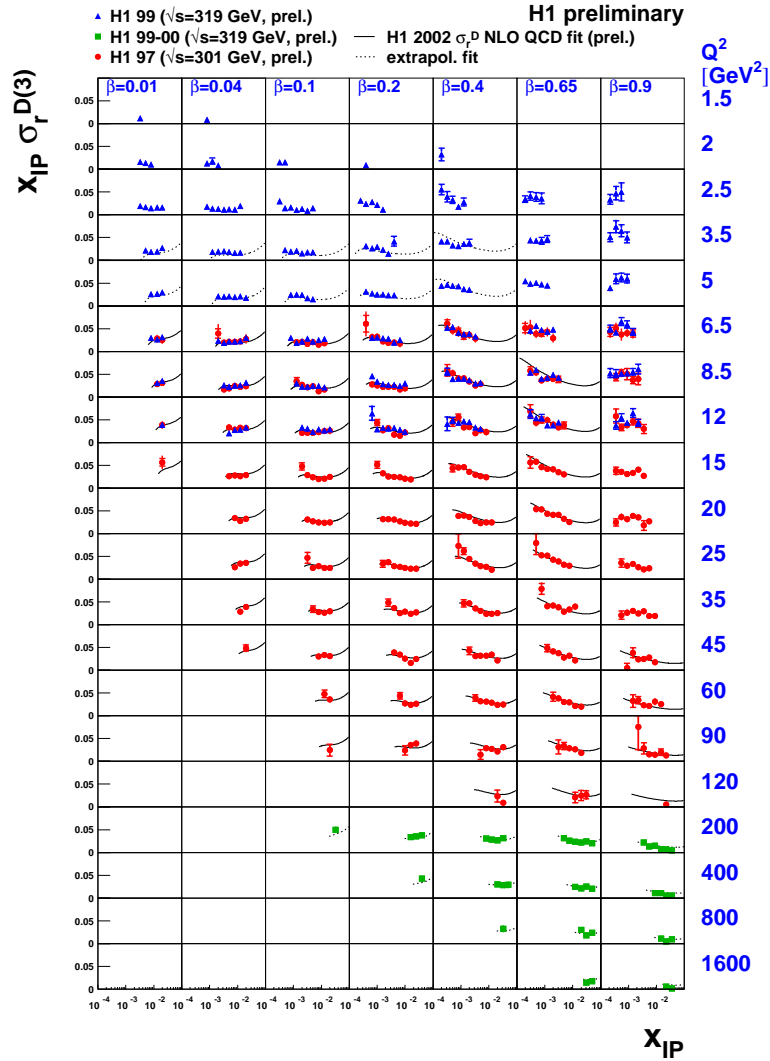


Fig. 3. Reduced diffractive cross section $x_{IP} \sigma_r^{D(3)}$ as function of x_{IP} . Also shown is the prediction from an NLO-QCD fit to the cross sections at medium Q^2 ($6.5 < Q^2 < 120$ GeV²). The dotted lines are extrapolations of this fit to lower and higher values of Q^2 .

were integrated over t (which is not measured for the high statistics samples using the M_X or rapidity gap methods, see Section 2). The results from the various methods of selecting diffractive events are consistent with each other and the data from ZEUS and H1 show good agreement in the commonly covered kinematic regions.

In comparison to standard inclusive DIS, diffractive deep-inelastic scattering (DDIS) has quite a number of similar features (data are not shown here, but see references given). Except for high β , corresponding to low M_X , the ratio of diffractive to inclusive cross sections is remarkably flat as function of W (and Q^2) when plotted at fixed x and $x_{\mathcal{P}}$. This implies a very similar energy dependence for the diffractive and inclusive γ^*p cross sections, most notably a strong rise of DDIS with W . In fact, from fits [9,12] to the data an intercept of an effective Regge trajectory is determined (H1 and ZEUS measure values around $\alpha_{\mathcal{P}} \sim 1.16 \pm 0.03$), incompatible with the universal “soft” Pomeron. The data are not yet precise enough, however, to firmly establish a dependence of $\alpha_{\mathcal{P}}$ on Q^2 . Fig. 4 shows the results of a Regge fit to the DDIS data from ZEUS [12], which indicate that the Regge factorization assumption (see Eq. (6)) is a valid approximation for values of $x_{\mathcal{P}} < 0.01$. For higher values of $x_{\mathcal{P}}$ subleading Reggeon contributions are expected and in fact required to describe the data [9].

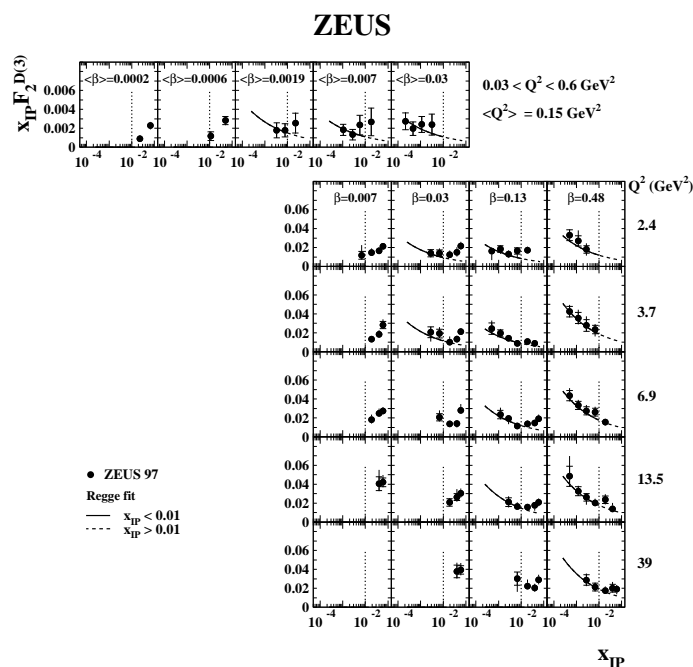


Fig. 4. ZEUS results [12] for the diffractive structure function $x_{\mathcal{P}} F_2^{D(3)}$ as a function of $x_{\mathcal{P}}$, for different values of β and Q^2 . The vertical lines indicate $x_{\mathcal{P}} = 0.01$. The solid line shows the results of a Regge fit assuming factorization. The dashed curves are extensions of the fit for $x_{\mathcal{P}} > 0.01$.

4. The partonic structure of diffraction

Fig. 5 shows the reduced cross section $x_{\mathbb{P}}\sigma_{\mathbb{r}}^{\text{D}(3)}$, measured by H1 [11], as a function of β at several values of Q^2 and at fixed $x_{\mathbb{P}}=0.01$. A remarkable feature of $x_{\mathbb{P}}\sigma_{\mathbb{r}}^{\text{D}(3)}$ (which is essentially $x_{\mathbb{P}}F_2^{\text{D}(3)}(\beta, Q^2)$) is the observed weak dependence on β . This is very much in contrast to the strong drop towards large x of $F_2(x, Q^2)$ in inclusive scattering (note that β in DDIS plays the role of x in DIS). The observed β dependence in DDIS is more similar to the photon structure functions (SF) than to the proton SF.

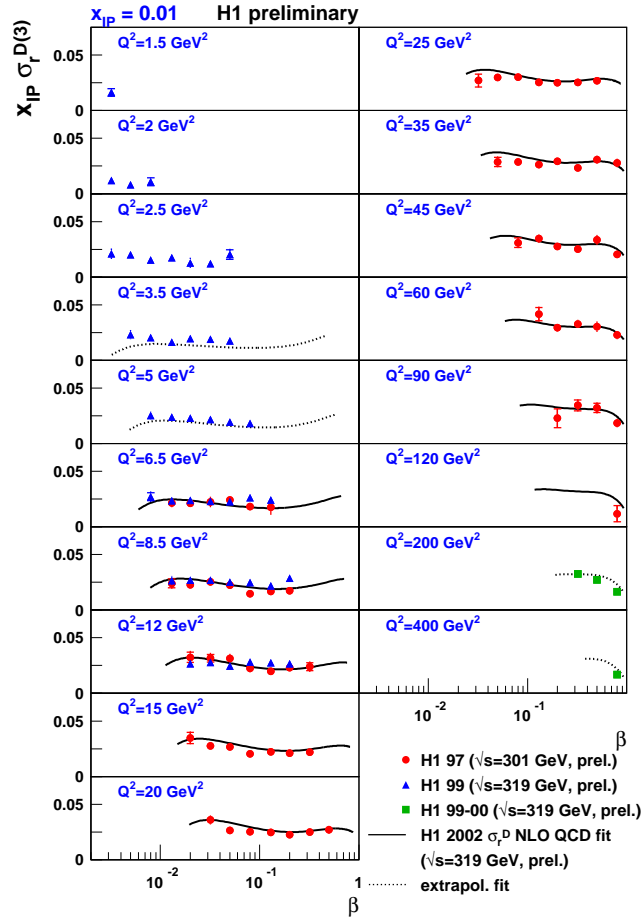


Fig. 5. Measurements of the reduced diffractive cross section $x_{\mathbb{P}}\sigma_{\mathbb{r}}^{\text{D}(3)}(x_{\mathbb{P}}, \beta, Q^2)$ as a function of β , in the Q^2 range of $1.5 < Q^2 < 400 \text{ GeV}^2$ from [9, 11], compared to a prediction from a NLO QCD fit performed to the Q^2 range $6.5 < Q^2 < 120 \text{ GeV}^2$ (solid lines, see text). The dotted lines correspond to extrapolations of the fit to lower and higher values of Q^2 .

Another remarkable feature of DDIS is observed in the Q^2 dependence of $x_{\mathbb{P}}\sigma_{\mathbb{P}}^{\text{D}(3)}$ for fixed values of β at $x_{\mathbb{P}} = 0.01$ (see Fig. 6). Here one clearly sees the expected scaling violations caused by strong gluon radiation. However, they are positive almost throughout the entire β interval. Only at large values of β ($\beta \geq 0.6$) the scaling violations become negative. Such details of the data should be naturally reflected in the parton distributions resulting from a QCD analysis and thus provide insight into the nature of the diffractive exchange.

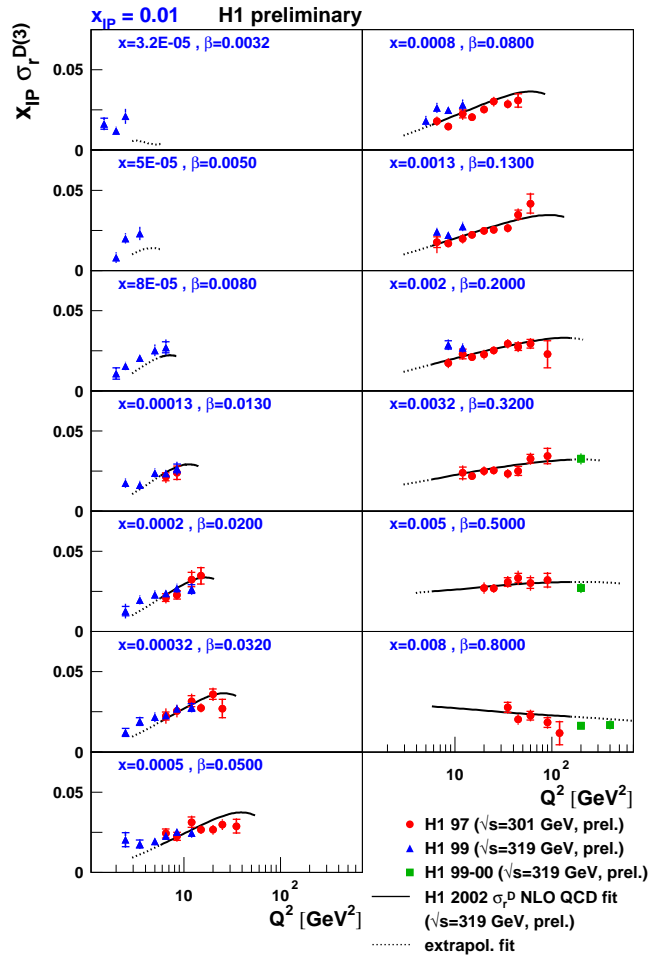


Fig. 6. Measurements of the reduced diffractive cross section $x_{\mathbb{P}}\sigma_{\mathbb{P}}^{\text{D}(3)}(x_{\mathbb{P}}, \beta, Q^2)$ as a function of Q^2 , in the β range of $0.0032 < \beta < 0.8$ from [9, 11], compared to a prediction from a NLO QCD fit performed to the Q^2 range $6.5 < Q^2 < 120$ GeV² (solid lines, see text). The dotted lines correspond to extrapolations of the fit to lower and higher values of Q^2 .

4.1. QCD analyses of diffractive data

With the experimental support of Regge factorization (within the present precision), QCD fits have been performed by the H1 Collaboration [9] in leading order (LO) and next-to-leading order (NLO), using the DGLAP formalism to evolve the non-perturbative diffractive parton densities (dpdf's). Similar fits were also done recently by the ZEUS Collaboration [12]. The dpdf's in both analyses are composed of a singlet of light quark flavors ($6 \cdot u$, where $u = d = s = \bar{u} = \bar{d} = \bar{s}$), and a gluon distribution, parameterized by a set of polynomials, at a scale $Q_0^2 = 3 \text{ GeV}^2$ in the case of H1. In the fits, the dpdf's are evolved using the DGLAP equations for $Q^2 > Q_0^2$ both in LO and NLO. The strong coupling constant α_s was fixed by setting $\Lambda_{\text{QCD}}^{\overline{\text{MS}}} = 0.2 \text{ GeV}$ and the charm quark is treated in the massive scheme via boson–gluon fusion processes with $m_c = 1.5 \pm 0.1 \text{ GeV}$. The normalization of the dpdf's is chosen so that the Pomeron flux factor is unity at $x_P = 0.003$. The result of the fit to the measurements of $x_P \sigma_r^{\text{D}(3)}$ in the regime $x_P < 0.01$ is shown in the Figs. 3, 5 and 6, and the corresponding dpdf's themselves are shown in Fig. 7. The error bands for the NLO dpdf's include the experimental and theoretical uncertainties, the latter being estimated from variations of m_c , Λ_{QCD} and the parameters used in the Pomeron flux factors. It is evident that the gluonic contributions dominate the partonic content and the

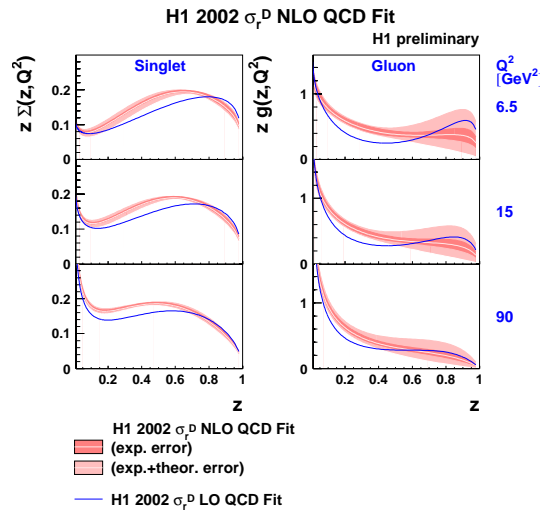


Fig. 7. Diffractive parton densities obtained from the QCD fits (see text) for various values of Q^2 . The left-hand side shows the singlet quark distribution, the right-hand side shows the gluon density. The bands show the results from the NLO fit, where the inner part represents the experimental, and the outer part represents the full error, including the theoretical uncertainties. For comparison the central values from the LO fit are also shown (solid line).

resulting momentum fraction carried by gluons amounts to about $75 \pm 15\%$ (ZEUS [13] arrive at a very similar conclusion concerning the gluon dominance in the diffractive pdf's). The H1 fit reproduces well all features of the data, most importantly the rising scaling violations which persist up to high values of β (see Fig. 6). This feature of a “late” turnover of the scaling violations in DDIS from positive to negative (at $\beta_s \sim 0.5$) is in contrast to the situation in DIS, where the turnover in the proton structure happens around $x_s \sim 0.15$. This fact may be explained by a conjecture we propose here that the turn-over point x_s (or β_s) is related to the average number n of constituent partons in a hadronic state by $x_s \sim 1/n$.

The physical motivation for this conjecture is the following: In lowest order (absence of gluon radiation) the n constituent partons within a hadronic state share their longitudinal momenta. So on average each parton carries the fraction $1/n$, corresponding to $x_s \sim 1/n$. Higher order processes (gluon radiation from these constituents) will distort the parton distributions by depopulating the region $x > x_s$ and populating the region $x < x_s$. Obviously the point x_s serves as a “fixed point”. For the case of diffractive exchange the intuitive lowest order picture is a 2-gluon intermediate state¹, well consistent with the observed $1/\beta_s \sim 2$.

5. Tests of factorization

Using the dpdf's obtained from the NLO QCD fits described above, one can perform a number of specific tests of the validity of the assumptions going into the QCD analysis. Most importantly, the QCD factorization theorem for DDIS can be tested. Since the gluon was shown to dominate, there is special interest in processes which are sensitive to photon–gluon interactions, such as $\gamma^* g \rightarrow q\bar{q}$, *i.e.* dijet and heavy flavor production (see Fig. 8). The longitudinal momentum fraction carried by the gluon emitted from the diffractive exchange, z_P , is determined using the invariant mass M_{12} of the $q\bar{q}$ system. In order to calculate a diffractive $q\bar{q}$ cross section (dijet or heavy quarks) in DIS, parton level calculations up to next-to-leading order are interfaced with the dpdf's obtained from the QCD fits. For the calculation of dijet and heavy flavor cross sections to NLO in QCD the programs DIS-ENT [14] and HVQDIS [15] were used. Hadronization corrections are then applied to the predictions, based on results from LO MC models.

¹ For the proton the constituent number would be about 6 ($n \simeq 1/0.15$), the three valence quarks, and three gluons (carrying 50% of the proton momentum), necessary to bind the quarks together.

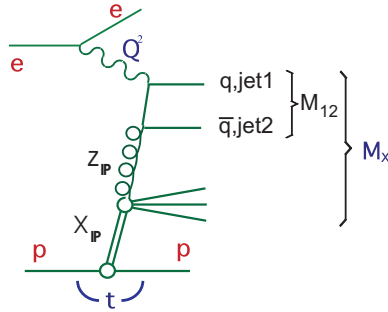


Fig. 8. Diagram for heavy quark or jet production in diffractive deep-inelastic scattering in the resolved Pomeron picture ($\gamma^* g \rightarrow q\bar{q}$, with invariant mass M_{12}). The gluon is emitted with longitudinal momentum fraction z_{IP} , which can be expressed as follows: $z_{IP} = (Q^2 + M_{12}^2)/(Q^2 + M_X^2)$.

5.1. Diffractive jet and charm production

Fig. 9, shows the differential cross section from H1 [16] for dijet production in DDIS as function of z_{IP} (for quark-induced processes at LO, z_{IP} is equivalent to β). The data are compared with LO and NLO calculations using DISSENT interfaced to the H1 dpdf's. Note that the predictions are corrected to the hadron level. The error band of the NLO calculations was estimated by varying the renormalization scale and taking into account the uncertainty of the hadronization correction. While the LO calculation misses by far, the NLO prediction describes the data, both in shape and normalization, within the experimental uncertainties.

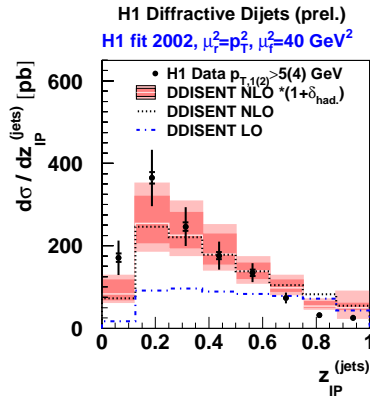


Fig. 9. Differential cross section for dijet production in diffractive DIS [16], corrected to asymmetric cuts on the jet transverse momentum $p_{T,1(2)} > 5(4)$ GeV, as a function of z_{IP} . The data are compared to predictions based on the H1 (N)LO dpdf's [9].

The ZEUS collaboration has recently measured open charm production in DDIS [13] using D^* -tagging (see Fig. 10). In the figure, the predictions from various models are shown, which generally are able to describe the measurements. In particular, the ACTW [17] NLO predictions, calculated from their gluon-dominated fit, give a reasonable account of the data. Similar conclusions have been reached by H1 [20].

ZEUS

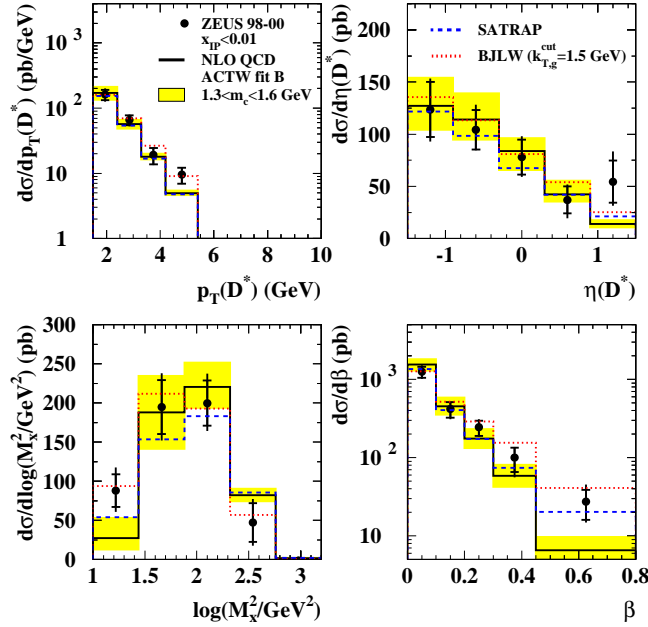


Fig. 10. Differential cross sections for diffractive D^* production (dots) in the kinematic range $1.5 < Q^2 < 200 \text{ GeV}^2$, $0.02 < y < 0.7$, $\beta < 0.8$, $p_T(D^*) > 1.5 \text{ GeV}$ and $|\eta(D^*)| < 1.5$, compared with several models [17–19]. The NLO prediction [17] based on gluon-dominated dpdf’s describes the data reasonably well. The shaded areas were obtained by varying the charm quark mass.

Both reactions, dijets and D^* production in DDIS, are reasonably well described by NLO calculations of the underlying photon–gluon fusion processes when convoluted with gluonic dpdf’s resulting from NLO fits to inclusive DDIS. This provides good support from the data that factorization for diffractive reactions holds indeed.

5.2. Diffractive photoproduction

As shown in the previous section, diffractive dijet (and charm) production is well described with NLO QCD fits to inclusive diffractive data. However, when a similar procedure is applied to diffractive jet production at the Tevatron, the observed rate is overestimated by one order of magnitude [21]. This breakdown of factorization was successfully explained, for example, by Kaidalov *et al.*, [23] as being caused by rescattering from the additional spectator quarks in the proton remnant, which are not present in virtual photon in DDIS.

In diffractive dijet photoproduction, on the other hand, there are two contributions, one where the photon directly participates in the hard scattering subprocess (“*direct photon*”), and another where a parton from the diffractive exchange scatters from a partonic fluctuation of the photon (“*resolved photon*”). The momentum fraction carried by the photon constituent in the resolved case is denoted by x_γ . Evidently, for the direct case x_γ is close to unity. The resolved photon part in dijet photoproduction is similar to hadron–hadron scattering and should, therefore, receive a suppression, similar to the $\bar{p}p$ case. Kaidalov *et al.*, [23] have indeed predicted a suppression factor $R \simeq 0.34$ for the resolved photon contribution in diffractive dijet photoproduction at HERA.

The H1 collaboration [22] has measured this process (see Fig. 11), requiring $E_T^{\text{jet}1} > 5 \text{ GeV}$ and $E_T^{\text{jet}2} > 4 \text{ GeV}$ for the two jets, which provide the hard scale necessary for comparisons with pQCD. The kinematic regime $Q^2 < 0.01 \text{ GeV}^2$ and $165 < W < 240 \text{ GeV}$ was chosen for the measurement of cross sections. The LO dpdf’s from the H1 fit [9], interfaced with the RAPGAP [24] Monte Carlo program are able to describe the data surprisingly well over the entire x_γ range, both in shape and normalization.

New LO and NLO calculations by Klasen and Kramer [25] lead to a somewhat different conclusion. Their NLO prediction overshoots the data and requires a suppression factor R . Choosing $R = 0.34$ for the resolved-photon part only, as suggested by Kaidalov *et al.*, Klasen and Kramer are in reasonable agreement with the data, although some details of the experimental input to correct the prediction for hadronization effects are questionable. Their LO prediction, on the other hand, in contrast to the LO prediction of RAPGAP (which includes parton showers and hadronization effects) shown in Fig. 11, is unable to describe the data, independently of the choice for R .

In a recent analysis H1 [26] use an NLO program by Frixione *et al.*, [27], interfaced to the H1 NLO dpdf’s, to predict the measured dijet photoproduction cross sections (for details of the implementation see [26]). The corresponding predictions² are shown in Fig. 11. As in the case for the Klasen

² The analyses [26] and [28] were not available at the time of the ISMD04 conference.

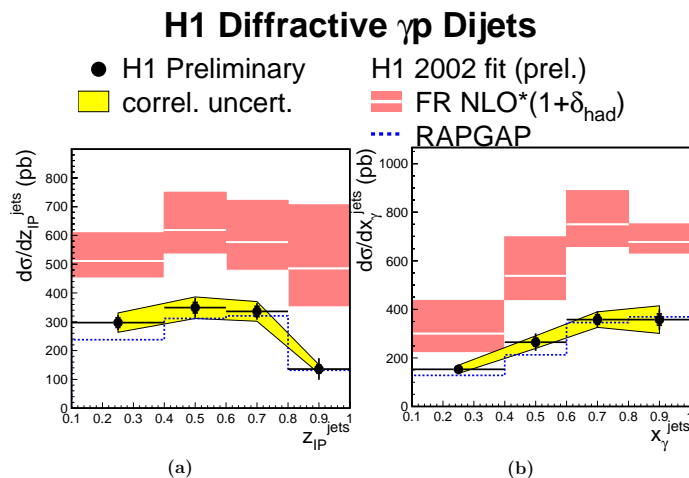


Fig. 11. Measurements [22, 26] by the H1 Collaboration of diffractive dijet cross sections in photoproduction as functions of $z_{\mathcal{P}}$ and x_{γ} . Also shown are the NLO predictions of a program by Frixione *et al.*, [27] interfaced to the H1 NLO dpdf's [9], and the RAPGAP prediction, which contains parton showers and is based on the LO dpdf's from H1. Both predictions include the effects of hadronization. The band around the NLO prediction indicates the uncertainty resulting from simultaneous variations of the renormalization and factorization scales by factors of 0.5 and 2.

and Kramer calculation, a clear overshoot is observed, requiring a suppression factor $R = 0.5 \pm 0.1$ to describe the measurements. It is interesting to note that for the H1 calculation both the direct and the resolved photon contributions need to be scaled down by the same factor. Similar findings were also obtained by the ZEUS collaboration [28], using the H1 dpdf's. Since the ratio of data to NLO predictions in dijet photoproduction is about a factor of 0.5 smaller than the same ratio in DIS, the breaking of QCD factorization in diffractive photoproduction has been demonstrated. However, it remains to be firmly established whether this suppression is global, *i.e.* affecting both the direct and resolved photon contributions, or whether, as theoretical models would suggest, only the resolved part is suppressed.

6. Summary and conclusions

Diffractive exchange governs the bulk of the total cross section in hadronic interactions and also contributes a substantial part to deep-inelastic electron–proton scattering at HERA. Based on a QCD factorization theorem for DDIS, the nature of the diffractive exchange can be studied through QCD fits to inclusive diffractive data. Such fits were carried out by both HERA

collaborations. The common conclusion is that diffractive exchange is dominated by gluons, contributing $(75 \pm 15\%)$. The form of the observed scaling violations hints towards the diffractive exchange being composed of a small number (~ 2) of partons. This is in agreement with the intuitive picture of a colorless two-gluon system mediating diffractive exchange in leading order. Using the dpdf's obtained from the LO and NLO QCD fits, the factorization assumption is tested successfully in the diffractive production of dijets and open charm. On the other hand, using the HERA diffractive parton distributions, a strong suppression of the cross section is required to explain the Tevatron diffractive dijet data. This suppression is quantitatively explained by rescattering effects of the spectator partons not involved in the hard scattering process. There is no clear picture yet for the diffractive dijet photoproduction at HERA, where a suppression would be expected for the resolved photon part. A measurement by H1, on the one hand, is correctly predicted using the dpdf's integrated into a LO QCD Monte Carlo model, while recent NLO calculations suggest suppression factors of order 0.5 for both the direct and resolved photons.

The author is very much indebted to the organizers of the ISMD04 conference for the excellent preparation and smooth running of the meeting on the Sonoma university campus, as well as for the very warm and relaxed, but nevertheless highly stimulating, atmosphere they were able to create. He also acknowledges the careful reading of the manuscript and the helpful suggestions by Hannes Jung and Paul R. Newman.

REFERENCES

- [1] H1 Collaboration, paper 984, submitted to ICHEP02, Amsterdam 2002.
- [2] ZEUS Collaboration, *Eur. Phys. J.* **C25**, 169 (2002).
- [3] A. Edin, G. Ingelman, J. Rathsman, *Phys. Lett.* **B366**, 371 (1996); J. Rathsman, *Phys. Lett.* **B452**, 364 (1999).
- [4] N.N. Nikolaev, B.G. Zakharov, *Z. Phys.* **C49**, 607 (1991); *Z. Phys.* **C53**, 331 (1992); A.H. Mueller, *Nucl. Phys.* **B415**, 373 (1994); W. Buchmüller, T. Gehrmann, A. Hebecker, *Nucl. Phys.* **B537**, 477 (1999); K. Golec-Biernat, M. Wüsthoff, *Phys. Rev.* **D59**, 14017 (1999); J. Bartels, K. Golec-Biernat, H. Kowalski, *Phys. Rev.* **D66**, 14001 (2002).
- [5] J. Collins, *Phys. Rev.* **D57**, 3051 (1998); *Phys. Rev.* **D61**, 19902 (2000).
- [6] G. Ingelman, P. Schlein, *Phys. Lett.* **B152**, 256 (1985).
- [7] P.D.B. Collins, *An Introduction to Regge Theory and High Energy Physics*, Cambridge University Press, Cambridge 1977; A. Donnachie, H.G. Dosch, P.V. Landshoff, O. Nachtmann, *Pomeron Physics and QCD*, Cambridge University Press, 2002, and references therein.

- [8] H1 Collaboration, C. Adloff *et al.*, *Z. Phys.* **C74**, 221 (1997).
- [9] H1 Collaboration, *Z. Phys.* **C76**, 613 (1997); papers 89 and 90, submitted to EPS 2003, Aachen, 2003; papers 908 and 981, submitted to ICHEP02, Amsterdam, 2002.
- [10] ZEUS Collaboration, *Z. Phys.* **C70**, 391 (1996); *Eur. Phys. J.* **C25**, 169 (2002); *Nucl. Phys.* **B658**, 2 (2003).
- [11] H1 Collaboration, paper 6-0175, submitted to ICHEP04, Beijing 2004.
- [12] ZEUS Collaboration, DESY preprint, DESY-04-131, August 2004.
- [13] ZEUS Collaboration, *Nucl. Phys.* **B672**, 3 (2003).
- [14] S. Catani, M.H. Seymour, *Nucl. Phys.* **B485**, 29 (1997).
- [15] B.W. Harris, J. Smith, *Phys. Rev.* **D57**, 2806 (1998).
- [16] H1 Collaboration, *Eur. Phys. J.* **C20**, 29 (2001).
- [17] L. Alvero *et al.*, *Phys. Rev.* **D59**, 074022 (1999).
- [18] K. Golec-Biernat, M. Wüsthoff, *Phys. Rev.* **D59**, 014017 (1999).
- [19] J. Bartels, H. Jung, M. Wüsthoff, *Eur. Phys. J.* **C11**, 111 (1999).
- [20] H1 Collaboration, paper 6-0178, submitted to ICHEP04, Beijing 2004.
- [21] CDF Collaboration, *Phys. Rev. Lett.* **84**, 5043 (2000).
- [22] H1 Collaboration, paper 87, submitted to EPS03, Aachen 2003.
- [23] A.B. Kaidalov, V.A. Khoze, A.D. Martin, M.G. Ryskin, *Eur. Phys. J.* **C21**, 521 (2001); *Phys. Lett.* **B567**, 61 (2003).
- [24] H. Jung, *Comput. Phys. Commun.* **86**, 147 (1995).
- [25] M. Klasen, G. Kramer, DESY preprint, DESY-04-011, August 2004.
- [26] H1 Collaboration, paper 6-0177, submitted to ICHEP04, Beijing 2004.
- [27] S. Frixione, Z. Kunszt, A. Signer, *Nucl. Phys.* **B467**, 399 (1996); S. Frixione, *Nucl. Phys.* **B507**, 295 (1997).
- [28] ZEUS Collaboration, paper 6-0249, submitted to ICHEP04, Beijing 2004.